

Anomalous 10-ns emission in Ce³⁺-doped Cs₃LuCl₆

P. Dorenbos, E.V.D. van Loef, and C.W.E. van Eijk

Interfaculty Reactor Institute, Delft University of Technology, Mekelweg 15, 2629 JB Delft, The Netherlands

K.W. Krämer and H.U. Güdel

University of Bern, Department of Chemistry and Biochemistry, Freiestrasse 3, 3000 Bern 9, Switzerland

(Received 19 May 2003; published 22 September 2003)

An emission at 281 nm with a 10.5 ns single exponential decay and a highly selective, narrow excitation region between 202 and 211 nm has been observed for Ce³⁺ doped in Cs₃LuCl₆. Wavelengths between 50–200 nm and longer than 215 nm have zero excitation efficiency. Excitation and emission spectra of Cs₃LuCl₆:Ce³⁺ in the 10–300 K temperature range were excited by pulsed synchrotron radiation between 50–335 nm. In addition to this new emission, the conventional Ce³⁺ doublet emission from the lowest 5*d* level to the ²F_{5/2} (368 nm) and ²F_{7/2} levels (400 nm) of the 4*f*¹ configuration is observed. Autoionization of the 5*d* electron to conduction band states followed by the direct transition to the ²F levels is proposed to explain the 281 nm emission and to explain the absence of emission under across bandgap excitation.

DOI: 10.1103/PhysRevB.68.125108

PACS number(s): 78.47.+p, 71.70.-d, 71.35.-y

I. INTRODUCTION

In the search for new inorganic scintillator materials for the detection of ionizing radiation, Ce³⁺ is often used as the optically active dopant. Free electrons and holes recombine at the Ce³⁺ center and the dipole allowed 5*d*→4*f* transition generates a fast (17–60 ns) decaying scintillation pulse. Much work has already been done on halide materials, and especially Ce³⁺ doped LaCl₃ and LaBr₃ have outstanding scintillation properties.^{1,2} Scintillation properties of Cs₃LuCl₆:Ce³⁺ have been reported by van 't Spijker.³ The high atomic numbers of Cs and Lu provide a host crystal ($\rho=3.8$ g/cm³) with a good stopping power for gamma rays. In this work we focus on the spectroscopic and luminescence properties. Ce³⁺ has a closed shell [Xe] configuration with one additional optically active electron in the 4*f* shell that is shielded from the crystalline environment by the filled 5*s*² and 5*p*⁶ shells of the [Xe] core. The shielding is absent in the excited [Xe]5*d* configuration, where the 5*d* electron experiences a strong interaction with the crystal field.

Ce³⁺ is located on a Lu³⁺ site in the center of a slightly distorted octahedron of six chlorine ions. The situation is quite similar to the elpasolites Cs₂NaLuCl₆ and Cs₂LiYCl₆. At the perfectly octahedral Lu and Y sites of the elpasolites, the 5*d* configuration splits into a lower 5*d*₁ state and an upper 5*d*₂ state separated by ≈ 2.5 eV.⁴ A similar splitting occurs in Cs₃LuCl₆:Ce³⁺, but in addition an emission with fast single exponential decay ($\tau=10.5$ ns) is observed around 281 nm. This emission is only excited by the 4*f*→5*d*₂ transitions at 204 and 209 nm, and not at any other wavelength. The total absence of the emission when exciting across the bandgap of the host crystal is particularly interesting because such a phenomenon has not been reported before. To understand this phenomenon, the thermal quenching behavior of the emission is studied. A model is proposed based on the location of the 5*d* levels relative to the conduction band. Excitation of the 5*d*₂ states is followed by relaxation to lower lying conduction band states followed by the direct transition to the ²F states of Ce³⁺.

II. EXPERIMENTAL

Two single crystals of Cs₃LuCl₆ doped with 0.1 and 1% Ce³⁺ were grown by the Bridgman technique using a moving furnace and a static vertical ampoule. CsCl, LuCl₃, and CeCl₃ were used as starting materials. CsCl (Merck, suprapur, 99.995%) was dried in vacuum at 200 °C. LuCl₃ and CeCl₃ were prepared from Lu₂O₃ (99.995%), CeO₂ (99.9999%), NH₄Cl (Merck, p.a., sublimed), and HCl (30% Merck, suprapur) according to Refs. 5,6. The Ce³⁺ concentration of the nominally 1% doped sample was determined by ICPS to be 0.81%. Experiments were performed on unpolished fragments cleaved from the original crystal boule.

Cs₃LuCl₆ has the same structure as Cs₃BiCl₆ and the low temperature modification of Cs₃LaCl₆.^{7,8} It crystallizes in space group *C*12/*c*1 (No. 15) with lattice parameters of $a=268.30$ pm, $b=81.00$ pm, $c=129.34$ pm, and $\beta=99.70^\circ$ at room temperature. There are two Lu³⁺ sites which are partially occupied by the 15 pm larger Ce³⁺ ion in statistically distribution. The Lu1 site at Wyckoff position 4*d* has *C*₁ inversion symmetry with Lu-Cl distances of 266.5, 269.1, and 272.0 pm and the Lu2 site at position 4*e* has *C*₂ point symmetry with Lu-Cl distances of 264.7, 269.3, and 272.8 pm. The slight deviation from perfect octahedral coordination, and the difference between both sites is very small.

Time resolved excitation spectra between 50 and 335 nm with 0.3 nm resolution at temperatures from 10 to 300 K were measured at the SUPERLUMI vacuum ultraviolet station of HASYLAB at the DESY synchrotron facility in Hamburg, Germany. The synchrotron operated in the multibunch mode with bunches separated by 200 ns. Three types of excitation and emission spectra were recorded. The “fast spectra” were obtained by monitoring the emitted light in a 10–12 ns wide window starting 1–2 ns after the excitation synchrotron pulse. The “slow spectra” were recorded in an 80–100 ns wide window starting after 75 ns delay. The “integral spectra” used all light emitted. The excitation spectra were corrected for the spectral shape of the excitation source by means of a Na-salicylate reference measurement at room temperature. For emission spectra, a monochromator with a

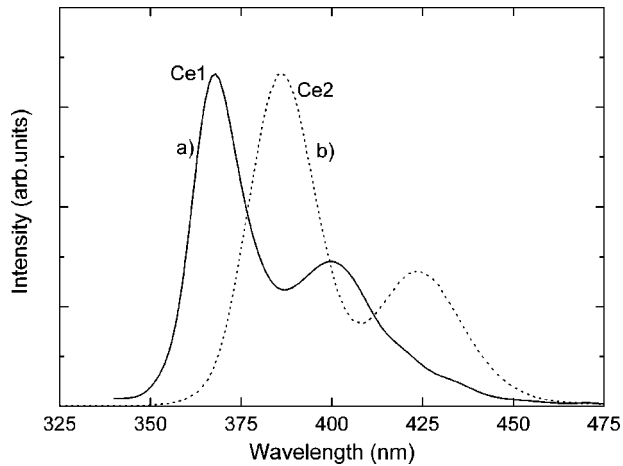


FIG. 1. (a) The Ce1 emission in $\text{Cs}_3\text{LuCl}_6:0.1\% \text{Ce}^{3+}$ under excitation into the $5d_i$ band at 328 nm. (b) The Ce2 emission in $\text{Cs}_3\text{LuCl}_6:0.81\% \text{Ce}^{3+}$ under excitation into the near defect exciton band at 185 nm. Spectra were taken at 10 K.

300 grooves/mm grating blazed in first order at 300 nm was used in combination with a photomultiplier tube. Emission spectra were not corrected for the detection efficiency of the system. Room temperature excitation and emission spectra at wavelengths longer than 330 nm were performed with a conventional UV/VIS spectrophotometer (Quanta Master QM1 of Photon Technology International).

III. RESULTS

Two different Ce^{3+} centers were identified in both samples. One center, hereafter referred to as Ce1, shows at 10 K the characteristic Ce^{3+} emission doublet at 368 and 400 nm, see Fig. 1. The emission of the other (Ce2) is shifted to longer wavelengths and maxima are found at 388 and 424 nm at 10 K. The emissions are due to the allowed transitions from the lowest $5d$ level to the ${}^2F_{5/2}$ and ${}^2F_{7/2}$ states of the $4f^1$ configuration. The spin orbit splitting between the two 2F multiplets for both Ce^{3+} centers is 0.27 eV which agrees with expectation.

Figure 2 shows the fast (a) and slow (b) excitation spectra of 380 nm emission in $\text{Cs}_3\text{LuCl}_6:0.1\% \text{Ce}^{3+}$ and the excitation spectrum (c) at 368 nm of Ce1 emission in $\text{Cs}_3\text{LuCl}_6:0.81\% \text{Ce}^{3+}$. For Ce^{3+} on a site with (distorted) octahedral coordination, one expects an excitation band at low energy due to the $5d_i$ levels and a band at high energy due to the $5d_e$ levels. The strong excitation at wavelengths longer than 310 nm is therefore attributed to transitions to the $5d_i$ levels. The doublet at 204 and 209 nm in spectrum (c) is ascribed to transitions into the $5d_e$ levels of the Ce1 center. Spectra (a) and (b) monitor simultaneously the Ce1 and more strongly the Ce2 excitation. An extra excitation band appears at 213 nm. This band together with an anticipated band around 209 nm is attributed to the $5d_e$ excitation of Ce2.

Intense excitation bands are found in spectrum (a) at 183 and 174 nm. Excitation at 185 nm yields exclusively Ce2 emission, see Fig. 1. Spectrum (c) shows that the excitation

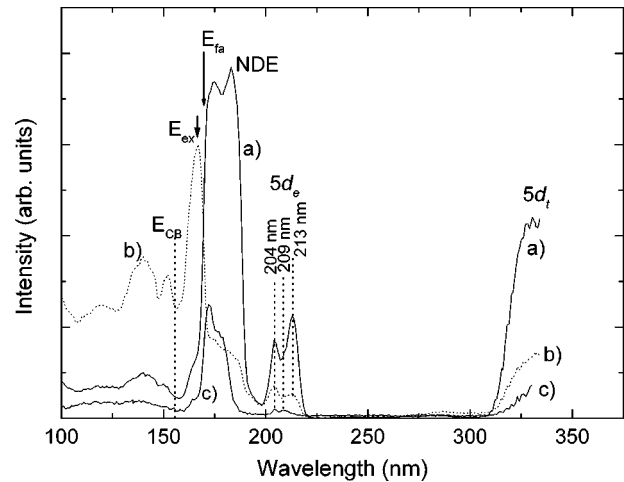


FIG. 2. Fast (a) and slow (b) excitation spectra of 380 nm emission in $\text{Cs}_3\text{LuCl}_6:0.81\% \text{Ce}^{3+}$. Spectrum (c) is the fast excitation spectrum of 370 nm emission in $\text{Cs}_3\text{LuCl}_6:0.81\% \text{Ce}^{3+}$. Spectra were taken at 10 K.

around 174 nm belongs to Ce1. There is a sharp threshold at 169 nm where the decay time of both Ce1 and Ce2 emissions change dramatically. At wavelengths longer than 169 nm the Ce^{3+} emission is fast and at shorter wavelengths the emission becomes very slow. The latter features are clearly related to excitations of the Cs_3LuCl_6 host crystal.

We attribute the peak at 166 nm in spectrum (b) to the exciton creation peak at energy $E_{ex}=7.47$ eV of the host lattice. Once created the excitons transfer energy to Ce1 and Ce2 relatively slowly. The location of the threshold is also clearly observed in other spectra. For example, for $\text{Cs}_3\text{LuCl}_6:0.81\% \text{Ce}^{3+}$ it is observed at 169 and 176 nm at 10 K and room temperature (RT), respectively. For $\text{Cs}_3\text{LuCl}_6:0.1\% \text{Ce}^{3+}$, the threshold is at 4 nm longer wavelength, i.e., at 173 and 180 nm. The shift to longer wavelength with increasing temperature is quite common for wide bandgap materials. Apparently there is also a small shift to longer wavelengths with decreasing Ce^{3+} concentration.

Figure 3 shows the UV/VIS excitation and emission spectra of $\text{Cs}_3\text{LuCl}_6:0.1\% \text{Ce}^{3+}$ at room temperature. Selecting different excitation wavelengths in the 320–380 nm region of the $5d_i$ band did not produce a significantly different emission spectrum. The emission peaks around 375 nm and the ${}^2F_{5/2}$ and ${}^2F_{7/2}$ emission bands are not resolved in the spectra, see spectrum (c). The emission is attributed to mainly Ce1 centers. Excitation in the leading edge at 360 nm [spectrum (a)] and the trailing edge at 430 nm [spectrum (b)] of the emission reveals the slightly shifted $5d_i$ bands of the weak Ce2 emission. We estimate the wavelengths of transition to the spin orbit split $5d_i$ state at 321 nm and $(2 \times)338$ nm for Ce1 and at 333 nm and $(2 \times)353$ nm for Ce2.

Figure 4 summarizes the energies and wavelengths involved in the Ce^{3+} and host lattice excitations. Taking the results for $\text{Cs}_3\text{LuCl}_6:0.1\% \text{Ce}^{3+}$ as a representative for the host crystal, we obtain a threshold $E_{FA}(10 \text{ K})=7.17$ eV and $E_{FA}(293 \text{ K})=6.89$ eV for the fundamental absorption of the host lattice. From the exciton peak energy at $E_{ex}=7.47$ eV, we estimate the bottom of the conduction band at around

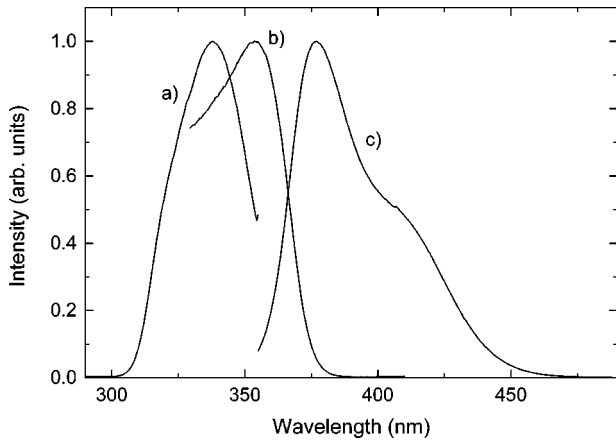


FIG. 3. UV/VIS excitation and emission spectra of Cs₃LuCl₆:0.1% Ce³⁺ at room temperature. Spectrum (a) and (b) are the excitation of emission at 360 and 430 nm, respectively. Spectrum (c) is the emission excited at 350 nm.

$E_{CB}=7.9$ eV which more or less coincides with a second threshold in spectrum (b) of Fig. 2. This estimate assumes a direct transition from the valence to the conduction band at the same point in the Brillouin zone where the exciton is created. Direct transitions at other points or indirect transitions might occur at lower energies.

Figure 5 shows decay time spectra of Ce1 and Ce2 emissions. Direct excitation at 320 nm into the $5d_t$ states, see spectrum (a), yields a single exponentially decaying Ce1 emission at 368 nm with $\tau=25$ ns. Excitation into the $5d_e$ state at 213 nm monitoring the Ce2 decay at 430 nm yields a

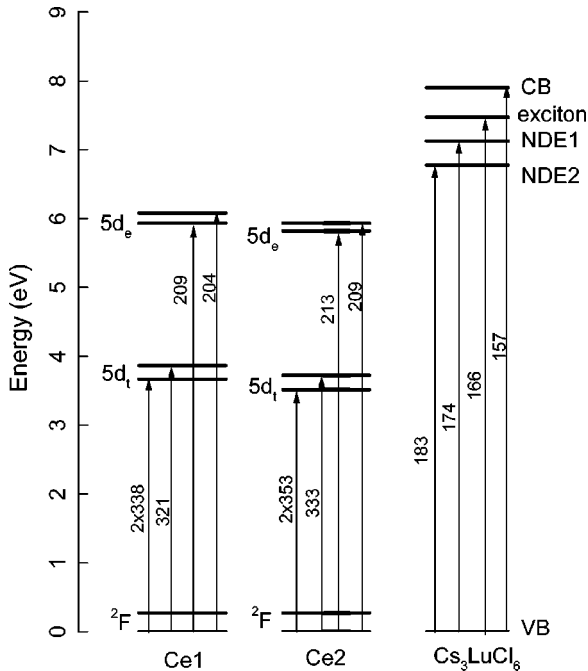


FIG. 4. Excitations identified in Ce1 and Ce2 centers starting from the $^2F_{5/2}$ ground state, and excitations in Cs₃LuCl₆:Ce³⁺ starting from the top of the valence band. The numbers along the arrows indicate wavelengths in nm.

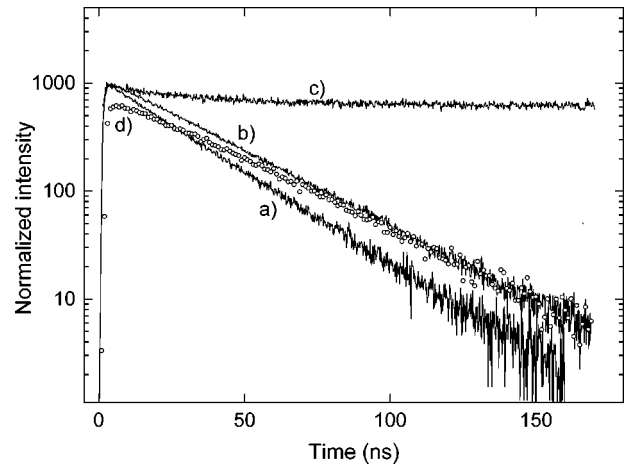


FIG. 5. Decay spectrum of (a) 368 nm Ce1 emission at 320 nm excitation in the $5d_t$ band. Decay (b) of 430 nm Ce2 emission at 213 nm excitation in $5d_e$. Decay (c) of 430 nm Ce2 emission at 165 nm excitation of the STE band. Decay (d) of 430 nm Ce2 emission at 328 nm excitation. (a) is for Cs₃LuCl₆:0.1% Ce³⁺ and (b), (c), and (d) for Cs₃LuCl₆:0.81% Ce³⁺. All at 10 K.

single exponential decay with $\tau=32$ ns, see spectrum (b). The same decay times are observed for excitations into the bands at 174 and 183 nm, respectively. On the other hand, excitation above the threshold into the exciton peak at 165 nm yields very slow emission of both Ce1 and Ce2, see spectrum (c). Curve (d) shows the Ce2 decay under excitation at 328 nm. The nonexponential shape of the curve in the first 50 ns indicates that (part of) the Ce2 emission is excited via energy transfer from the $5d_t$ level of Ce1.

So far all spectroscopic properties appear normal and can be interpreted with standard methods and ideas. Figure 6 shows emission spectra at 207.5 nm excitation corresponding to $5d_e$ excitation of dominantly Ce1 but also Ce2 in Cs₃LuCl₆:0.81% Ce³⁺. As expected, a mix of Ce1 and Ce2 emissions is observed in the 350–450 nm region. Ce1 domi-

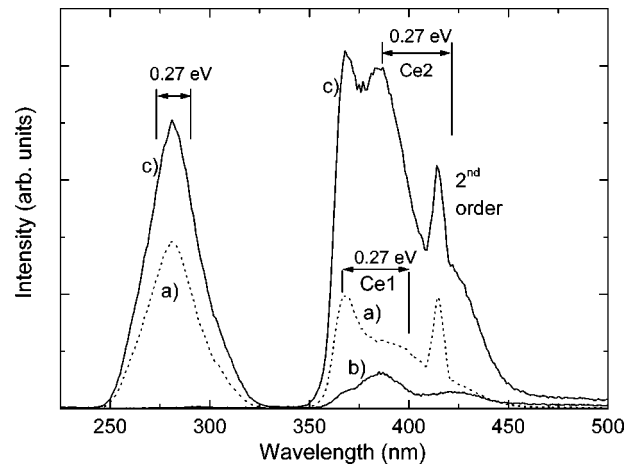


FIG. 6. Fast (a), slow (b), and integral (c) emission spectra excited at 207.5 nm into the $5d_e$ levels of Ce1 and Ce2 in Cs₃LuCl₆:0.81% Ce³⁺ at 10 K. The peak at 415 nm is an artifact due to second order transmission of the monochromator.

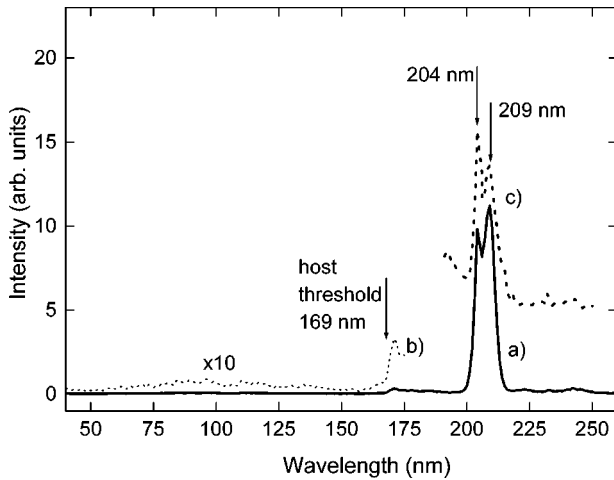


FIG. 7. Fast excitation spectrum (a) of the 281 nm anomalous emission in $\text{Cs}_3\text{LuCl}_6:0.81\% \text{Ce}^{3+}$ at 10 K. The wavelength region up to 175 nm is shown (b) with 10 times enlarged scale. Spectrum (c) is part of the excitation spectrum of 368 nm Ce1 emission in $\text{Cs}_3\text{LuCl}_6:0.1\% \text{Ce}^{3+}$ at 10 K. The arrow at 169 nm indicates the threshold of the fundamental absorption of the host lattice.

nates in the fast spectrum (a) and Ce2 in the slow one (b). In addition a fast broad (0.46 eV FWHM) emission band is centered at 281 nm.

Figure 7 shows the excitation spectrum of the 281 nm emission. The two excitation bands at 204 nm and 209 nm coincide exactly with the $5d_e$ levels of the Ce1 center, see spectrum (c) in Figs. 7 and 2. The weak features between 170 and 200 nm and at wavelengths longer than 215 nm do not excite the main 281 nm emission band but are instead related to other weak emissions underneath this band. Also excitation of the Ce2 $5d_e$ band at 213 nm does not generate the 281 nm emission. Surprisingly, the 281 nm emission is not excited at wavelengths shorter than the fundamental absorption threshold at 169 nm of Cs_3LuCl_6 . We conclude that an excitation of the host crystal is not transferred to the state from which the anomalous 281 nm emission originates. Such a behavior is quite special and has not been reported before for Ce^{3+} doped materials. Usually, under host excitation always some energy transfer is observed.

Figure 8 shows the intensity of the anomalous emission at 281 nm and of the Ce1 emission at 368 nm as function of temperature. With increasing temperature the 281 nm emission quenches and fully disappears at 130 K, see curve (a). At the same time the intensity of the df emission of Ce1 increases, see curve (b). The drop of the Ce1 emission between 80 and 90 K is probably an artifact due to the change of instrumental parameters.

Figure 9 shows the decay spectra of the 260–320 nm emission as a function of temperature. At 12 K the decay is single exponential with $\tau=10.5$ ns. Together with the quenching of the emission intensity, the decay rate of the anomalous emission also increases, especially in the first 20 ns time window. The lifetimes τ of the fast component are shown as curve (c) in Fig. 8. The respective single exponential fits are added as broken lines in Fig. 9.

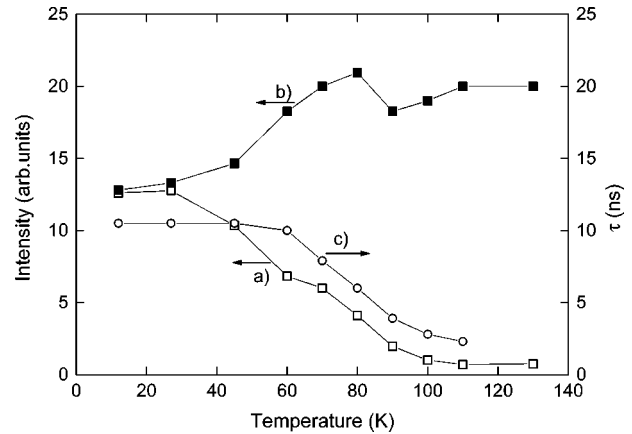


FIG. 8. Temperature dependence of the anomalous emission intensity at 281 nm (a) and the Ce1 emission intensity at 368 nm (b) of the fast spectrum for $\text{Cs}_3\text{LuCl}_6:0.1\% \text{Ce}^{3+}$. Curve (c) is the temperature dependence of the decay time τ (ns) of the anomalous emission at 281 nm.

IV. DISCUSSION

For Ce^{3+} located on a site of O_h point symmetry, the $5d$ configuration splits into a low energy triplet $5d_t$ state and a high energy doublet $5d_e$ state. The spin orbit interaction further splits the $5d_t$ state into a doublet plus a singlet at typically 0.12 eV higher energy. Table I compiles the energies of the $5d$ levels of Ce^{3+} in the elpasolite crystals $\text{Cs}_2\text{LiYCl}_6$ and $\text{Cs}_2\text{NaLuCl}_6$. Although, the sites in the undistorted lattice are of perfect O_h symmetry, a clear splitting of the high energy e_g doublet is observed. It is probably caused by symmetry lowering due to lattice relaxation or the Jahn-Teller effect.

Despite the fact that the two Lu sites in Cs_3LuCl_6 are of lower symmetry than O_h , the deviation from the pure octahedral crystal field splitting is not large. Table I shows that

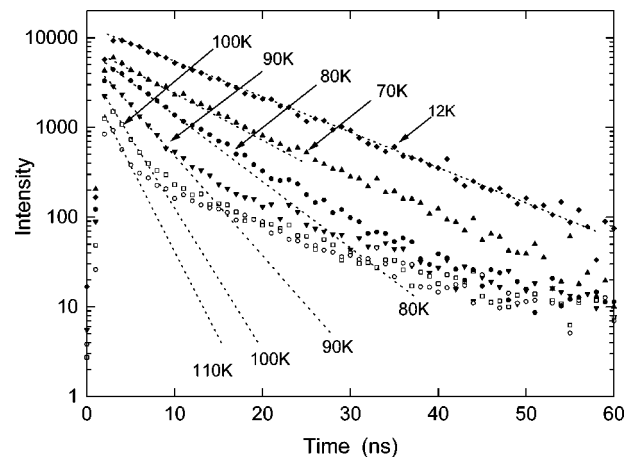


FIG. 9. Decay spectra of 281 nm anomalous emission in $\text{Cs}_3\text{LuCl}_6:0.1\% \text{Ce}^{3+}$ as function of temperature. The spectra are normalized in a way that the integral number of counts in the 4–17 ns interval scales with the intensity of the 281 nm emission band. The straight, broken lines indicate the fast decay component in the first 20 ns.

TABLE I. Energy E_i of the five $5d_i$ levels of Ce³⁺ in two elpasolite crystals and in Cs₃LuCl₆. E_{FA} is the energy of the fundamental absorption and E_{CB} the estimated energy of the conduction band. All energies are in eV. R_{av} is the average Lu-Cl or Y-Cl distance in pm.

Compound	R_{av}	E_5	E_4	E_3	E_2+E_1	E_{FA}	E_{CB}
Cs ₂ LiYCl ₆	263	5.90	5.74	3.79	(2x)3.55	6.60	
Cs ₂ NaLuCl ₆	≈259	5.96	5.74	3.70	(2x)3.54	6.95	
Cs ₃ LuCl ₆ :Ce1	269	6.08	5.93	3.86	(2x)3.65	6.90	7.9
Cs ₃ LuCl ₆ :Ce2	269	5.96	5.82	3.72	(2x)3.51	6.90	7.9

the level energies for Ce1 and Ce2 compare well with those for Ce³⁺ in the elpasolites.

It is tempting to identify the Ce1 and Ce2 centers as belonging to the two crystallographically distinct Lu sites in Cs₃LuCl₆. However, the sites are not much different and similar energies for the $5d$ levels of the two sites are expected. Furthermore the intensity of the Ce2 related emission in the 0.1% Ce³⁺ doped sample is much weaker than in the sample with 0.81% Ce³⁺. We therefore conclude that the Ce1 center belongs to Ce³⁺ on both Lu sites, and the spectroscopic properties at the two sites are not significantly different. Ce2 is assigned to a disturbed Ce center, most likely due to the presence of other nearby Ce³⁺ ions.

The intense excitation bands at 174 nm for Ce1 and 183 nm for Ce2 are attributed to so-called near defect excitons (NDE's). Such excitations are often observed at energies just lower than the exciton peak of the undistorted host crystal.^{9–11} Since the excitation is located close to a Ce³⁺ defect, an almost instantaneous (faster than 1 ns) energy transfer to Ce³⁺ occurs leading to Ce³⁺ emission with the same decay time as for direct $5d$ level excitation.

Figure 10 shows a configuration coordinate model for the anomalous emission. The bottom of the conduction band, the host exciton level, and the near Ce1 defect exciton level (NDE1) are located at 7.9, 7.47, and 7.17 eV; see also Fig. 4. Information on the location of the Ce³⁺ levels relative to the

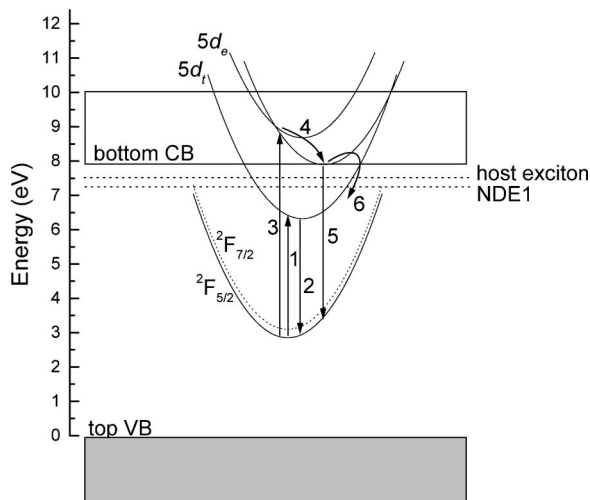


FIG. 10. Energy level scheme of Ce³⁺ in Cs₃LuCl₆. The transitions indicated by the numbered arrows are explained in the text.

conduction band or the valence band is not available for Cs₃LuCl₆. However, we can give an estimate based on (1) From x-ray photoelectron spectroscopy on CeCl₃ it is known that the $4f^1[{}^2F_{5/2}]$ ground state of Ce³⁺ is located ≈2 eV above the top of the chlorine valence band.¹² (2) The energy of charge transfer E_{CT} of an electron from the valence band to Eu³⁺ increases with smaller anion coordination number and shorter distance to the anions.^{13,14} (3) The conduction band energy E_{CB} of Ln³⁺ compounds increases with smaller size of the lanthanide ion. (2) and (3) are explained by the shorter distance to the negative anions leading to a more negative Madelung potential at that site. All electron levels of impurity and conduction band states raise relative to the valence band.¹⁵ The difference in E_{CT} and E_{CB} between La compounds and Lu compounds is usually 0.7–1.0 eV. Adding this difference to the ≈2 eV from the XPS data on CeCl₃, we estimate the energy of the $4f$ ground state of Ce³⁺ at 2.9 eV above the valence band of Cs₃LuCl₆. This situation is sketched in Fig. 10. We arrive at a situation where the $5d_t$ state is well below the bottom of the conduction band and the $5d_e$ state is placed within the conduction band.

We envisage the following mechanisms: An excitation into the $5d_t$ levels (arrow 1) yields normal 0.28 eV Stokes shifted Ce³⁺ emission with single exponential decay (arrow 2). An excitation into the $5d_e$ levels (arrow 3) can be followed by different steps. The $5d_e$ state can decay by multiphonon relaxation to the $5d_t$ states followed by normal df emission (arrow 2). In most Ce³⁺ doped compounds this nonradiative process is very fast (<1 ns) and leads to a single exponential decay regardless which of the $5d$ levels was excited. For Cs₃LuCl₆ the situation is special because of the large energy gap of 2.07 eV between the lowest $5d_e$ state and the highest $5d_t$ state. Furthermore the maximum phonon frequency in chlorides is small. Both together prevent the fast multi-phonon relaxation to the $5d_t$ states. Furthermore, a radiative decay from $5d_e$ to the $5d_t$ states is forbidden.

Much more likely is the autoionization of the $5d_e$ electron to the conduction band (arrow 4) where the electron remains localized in the attractive Coulomb potential around the Ce ion. The emission at 281 nm is now attributed to the direct recombination of this state with the hole left behind on Ce (arrow 5). Essentially, this process is a dipole allowed charge transfer in agreement with the observed fast exponential decay of 10.5 ns. Due to the 0.27 eV spin orbit splitting of the Ce³⁺ 2F state one may expect two emission bands around 281 nm. But the large offset between the excited and ground state parabolas in the configuration coordinate diagram leads to two broad overlapping emission bands in good agreement with the observed width of 0.46 eV (full width at half maximum).

The situation sketched above is similar to the impurity trapped exciton emission sometimes observed for Eu²⁺ and Yb²⁺.^{15,16} Whenever the lowest $4f^{n-1}5d$ state of these lanthanides is located close to the bottom of the conduction band, the electron in this state tends to autoionize to the conduction band, but remains bonded to the lanthanide ion. An impurity trapped exciton configuration is obtained lead-

ing to an emission with a large Stokes shift.

The essential difference between this situation and that of Ce^{3+} doped in Cs_3LuCl_6 is the presence of $5d_i$ states below the impurity trapped exciton state. It provides a route for thermal quenching of the anomalous emission (arrow 6). The anticorrelation between the 281 nm emission and the normal df emission intensity in Fig. 8 and the shortening of the decay time in Fig. 9 is fully in line with such a quenching model.

The anomalous 281 nm emission is not excited at wavelengths shorter than 169 nm. Apparently, free electrons in the conduction band and free holes in the valence band never recombine into the state that leads to the 281 nm emission. We can think of two mechanisms. (1) The hole is trapped first by Ce^{3+} . Ce^{4+} is created, and because its ionic radius is 18 pm smaller than that of Ce^{3+} there is a strong lattice relaxation. Next, the conduction band electron is trapped by Ce^{4+} , and again there is a strong lattice relaxation. The offsets in the configuration coordinate diagram are then much larger than sketched in Fig. 10, and the state responsible for the 281 nm emission, if it exists at all, immediately decays to the lowest $5d_i$ state. (2) The hole is trapped by the lattice to form a V_k -like center.¹¹ Next an electron is trapped by the V_k center to form a self-trapped exciton (STE). The STE does not have sufficient energy to excite the 281 nm emission, but instead transfers its energy to the $5d_i$ state of Ce^{3+} .

V. CONCLUSIONS

The spectroscopy of Ce^{3+} doped Cs_3LuCl_6 was studied between 10 and 300 K in the 50 to 375 nm region. Two Ce^{3+}

centers were identified. The Ce1 center is associated with an isolated Ce^{3+} ion on a Lu site. The other, that becomes more abundant at higher Ce concentration, is attributed to a disturbed Ce site. The energies of the $5d_i$ and $5d_e$ states of Ce1 are in line with expectations based on chloride elpasolite compounds with sixfold octahedral coordination polyhedra. At low temperature, the excitation into the $5d_e$ levels 204 and 209 nm yields, in addition to normal df emission, a fast emission ($\tau=10.5$ ns) at 281 nm. Upon heating, its intensity is quenched and its decay rate increases due to energy transfer to the Ce^{3+} $5d_i$ states. The fast emission vanishes at 130 K. Autoionization of the $5d_e$ electron to conduction band states, followed by a direct transition to the Ce^{3+2F} levels is proposed as model for the anomalous emission.

Most peculiar is the total absence of excitation efficiency for the 281 nm emission at energies above the fundamental absorption of the host crystal. This makes $\text{Cs}_3\text{LuCl}_6:\text{Ce}^{3+}$ a highly selective sensor for 202–211 nm ultraviolet light.

ACKNOWLEDGMENTS

The authors are grateful to Dr. M. Kirm (HASYLAB, DESY Hamburg) for his assistance in the experiments performed at the SUPERLUMI setup, to Dr. M.S. Wickleder for the synthesis of one of the samples used for study, and to Dr. E. van der Kolk for the UV/VIS measurements. These investigations were supported by the Dutch Technology Foundation (STW), the Swiss National Science Foundation, and by the IHP Contract No. HPRI-CT-1999-00040 of the European Commission.

¹E.V.D. van Loef, P. Dorenbos, C.W.E. van Eijk, K. Krämer, and H.U. Güdel, *Appl. Phys. Lett.* **77**, 1467 (2000).

²E.V.D. van Loef, P. Dorenbos, C.W.E. van Eijk, K. Krämer, and H.U. Güdel, *Appl. Phys. Lett.* **79**, 1573 (2001).

³J.C. van't Spijker, Ph.D. thesis, Delft University of Technology, The Netherlands, 1999.

⁴P. Dorenbos, *Phys. Rev. B* **62**, 15 650 (2000).

⁵G. Meyer, *Inorg. Synth.* **25**, 146 (1989).

⁶J.B. Reed, B.S. Hopkins, and L.F. Audrieth, *Inorg. Synth.* **1**, 28 (1936).

⁷F. Benachenhou, G. Mairesse, G. Nowogrock, and D. Thomas, *J. Solid State Chem.* **65**, 13 (1986).

⁸H.J. Seifert, H. Fink, and B. Baumgartner, *J. Solid State Chem.* **107**, 19 (1993).

⁹A. Lushchik, M. Kirm, A. Kotlov, P. Liblik, Ch. Lushchik, A. Maaros, V. Nagirnyi, T. Savikhina, and G. Zimmerer, *J. Lumin.* **102-103**, 38 (2003).

¹⁰E. Radzhabov, A.I. Nepomnyashikh, and A. Egranov, *J. Phys.: Condens. Matter* **14**, 7337 (2002).

¹¹K.S. Song and R.T. Williams, *Self-trapped Excitons*, Vol. 105 of Springer Series in Solid State Sciences (Springer-Verlag, Berlin, 1993).

¹²S. Sato, *J. Phys. Soc. Jpn.* **41**, 913 (1976).

¹³H.E. Hoefdraad, *J. Solid State Chem.* **15**, 175 (1975).

¹⁴G. Blasse, *Struct. Bonding (Berlin)* **26**, 43 (1976).

¹⁵P. Dorenbos, *J. Phys.: Condens. Matter* **15**, 2645 (2003).

¹⁶D.S. McClure and C. Pedrini, *Phys. Rev. B* **32**, 8465 (1985).